

were placed in a quartz cell and irradiated at 366 nm with a 500-W Hg lamp. The absorption peaks at 247 and 343 nm due to the *trans*-azobenzene unit disappeared, and a new peak of the *cis* isomer appeared at ca. 450 nm, consistent with the literature data.^{21a} The reverse (*cis*-to-*trans*) isomerization could be induced thermally or by irradiation at 450 nm. Therefore, clean, reversible *cis*-*trans* isomerization is induced by photochemical and thermal means. The photostationary state with the 366-nm light was attained in less than 10 min under the conditions used.

The isomerization is accompanied by the change in the aggregate morphology. The *trans* isomers of **2** are shown by electron microscopy to assemble in water to globular aggregates with diameters of ca. 200 Å (see Figure 3a).²³ The fine structure of these aggregates cannot be seen clearly; however, the observation of the phase transition²⁴ strongly suggests the presence of local molecular ordering (bilayers). Upon irradiation, the globular aggregate is transformed to the short rods (diameter 50–70 Å) of Figure 3b. The isomer ratio (*trans*/*cis*) of the latter was 55:45. The aggregate weight was 5.3×10^5 after irradiation, and, therefore, the aggregate size does not change essentially in spite of the morphology change. Further irradiation at 450 nm (*cis*-to-*trans* isomerization) produced the original globular morphology. Similar, reversible isomerization and morphology change were observed with the other azobenzene-containing amphiphiles (**2**, $n = 2, 10$).

The isomerization process is influenced by the physical state of the bilayer aggregate. The *cis* fraction at the photostationary state increased from 0.2 to 0.5 abruptly at 40–50 °C in the case of **2** ($n = 10$), corresponding to its phase transition ($T_c = 46$ °C). Its thermal (*cis*-to-*trans*) isomerization showed similarly peculiar behavior, and the Arrhenius plots of the initial rate were composed of two lines with an inflection near $T_c: E_a = 21$ and 27 kcal/mol and $\Delta S = -4$ and 11 eu in the temperature range below 35 °C and above 45 °C, respectively.

In conclusion, the present study establishes that the bilayer characteristics can be used for designing novel functions. The chromophore-containing bilayer should find many applications in fundamental and practical research.

Acknowledgment. We are grateful to Professors M. Takayanagi and K. Yamafuji for the use of an electron microscope and a spectropolarimeter, respectively.

(23) The amphiphile solution as prepared by sonication (and the subsequent aging in an ice bath for 30 min) was mixed with an equal volume of 2% aqueous uranyl acetate, sonicated for 10–20 s, and applied to carbon-coated Cu grids for electron microscopy (Hitachi Model H-500). The photoisomerization was performed with and without uranyl acetate. The resulting morphologies were the same.

(24) The phase-transition temperature, T_c , was determined by differential scanning calorimetry (Daini Seikoshu Model SSC/560) for 30 mM aqueous solutions; $T_c = 16, 25,$ and 46 °C for **2** ($n = 2, 4,$ and 10), respectively.

T. Kunitake,* N. Nakashima, M. Shimomura, Y. Okahata
Department of Organic Synthesis, Faculty of Engineering
Kyushu University, Fukuoka, 812, Japan

K. Kano, T. Ogawa
Department of Molecular Science and Technology
Graduate School of Engineering Sciences
Kyushu University, Fukuoka, 812, Japan

Received March 11, 1980

Successful Isolation of a Reduced Tetrathiometalate Complex. Synthesis and Structural Characterization of the $[(\text{MoS}_4)_2\text{Fe}]^{3-}$ Trianion

Sir:

The extended X-ray absorption fine structures (EXAFS) of the Mo centers in the Fe–Mo protein component of certain nitrogenases¹ and in the Fe–Mo cofactor^{1,2} have been obtained and

analyzed. The results of these analyses indicate that the Mo atom is situated at close proximity to four or five sulfur atoms at 2.36 Å and to two or three iron atoms at ~ 2.7 Å.

Recent attempts toward the synthesis of Fe–Mo–S analogue complexes have resulted in the isolation of two types of multinuclear aggregates which appear to be in relative compliance with the structural constraints imposed by EXAFS studies. These two types of Fe–Mo–S complexes are the Mo_2Fe_6 “double cubanes” and certain Fe complexes with MoS_4^{2-} as a ligand. In the double-cubane cluster complexes $[\text{Mo}_2\text{Fe}_6\text{S}_9(\text{SEt})_8]^{3-3}$ and $[\text{Mo}_2\text{Fe}_6\text{S}_8(\text{SR})_9]^{3-}$ ($\text{R} = \text{Et}, \text{Ph},^4$ and $\text{SCH}_2\text{CH}_2\text{OH}^5$), the Mo atoms are coordinated to six sulfur atoms with Mo–S bond lengths ranging from 2.35 to 2.57 Å.³ At a close proximity to the Mo atoms also are found three iron atoms at ~ 2.7 Å. From the recently reported Fe– MoS_4 complexes,⁶ the $[\text{Cl}_2\text{FeS}_2\text{MoS}_2\text{FeCl}_2]^{2-}$ anion^{6b} contains a central MoS_4^{2-} unit (Mo–S ~ 2.20 Å) bridging two FeCl_2 fragments with a Mo–Fe distance of ~ 2.8 Å. The presence of MoS_4^{2-} in the latter complex may be a relevant structural feature, to the extent that MoS_4^{2-} also may be present in nitrogenase. This contention finds support in a recent study of the Fe–Mo protein component from *Clostridium pasteurianum*. The results of this study indicate that MoS_4^{2-} is released following acid hydrolysis of the Fe–Mo protein. The possibility that a MoS_4 unit may be involved in coordination to Fe atoms in the active site of nitrogenase prompted us to examine further the coordination properties of the MoS_4^{2-} ligand.

The tetrathiometalate anions, MS_4^{2-} ($\text{M} = \text{Mo}, \text{W}$), as “ligands”⁸ are unique to the extent that in addition to the sulfur donor atoms they contain metal atoms with vacant d orbitals. Upon chelation, the MS_4 units bridge the Mo or W ions (formally in the 6+ oxidation state) within a relatively short distance (2.7–2.9 Å) from the chelated metal ion (M'). As expected, and suggested previously,⁹ overlap between the d functions of the M' ions and those of the Mo or W ions could result in $\text{M}' \rightarrow \text{M}(\text{VI})$ charge delocalization. The ability of the MS_4^{2-} anions to facilitate a delocalization of electrons is aptly illustrated in the remarkable redox properties of the $[(\text{MS}_4)_2\text{M}']^{2-}$ complexes ($\text{M} = \text{Mo}, \text{W}$; $\text{M}' = \text{Ni}, \text{Pd}$)¹⁰ and more recently of the $[(\text{WS}_4)_2\text{Co}]^{2-}$ complex.¹¹ In all of these complexes, two one-electron reversible reductions are observed.

As an extension of our studies on the MoS_4 –Fe complexes, we proceeded with a reinvestigation of the synthesis and properties of the $[(\text{MoS}_4)_2\text{Fe}]^{2-}$ complex anion. This compound was reported previously⁹ as an X-ray-amorphous material and was not characterized extensively because of its assumed questionable purity.

In this communication, we report on the synthesis and structural characterization of the new $[(\text{MoS}_4)_2\text{Fe}]^{3-}$ complex. We obtained this complex in microcrystalline form, in good yields and analytically pure, as the tris(tetraethylammonium) and tris(tetramethylammonium) salts. Specifically, the reaction of a concen-

(1) (a) S. P. Cramer, K. O. Hodgson, W. O. Gillum, and L. E. Mortenson, *J. Am. Chem. Soc.*, **100**, 3398 (1978); (b) S. P. Cramer, W. O. Gillum, K. O. Hodgson, L. E. Mortenson, E. I. Stiefel, J. R. Chrisnell, W. J. Brill, and V. K. Shah, *ibid.*, **100**, 3814 (1978).

(2) V. K. Shah and W. J. Brill, *Proc. Natl. Acad. Sci. U.S.A.*, **74**, 3249 (1977).

(3) (a) T. E. Wolff, J. M. Berg, C. Warrick, K. O. Hodgson, R. H. Holm, and R. B. Frankel, *J. Am. Chem. Soc.*, **100**, 4630 (1978); (b) T. E. Wolff, J. M. Berg, K. O. Hodgson, R. B. Frankel, and R. H. Holm, *ibid.*, **101**, 4140 (1979).

(4) (a) G. Christou, C. D. Garner, F. E. Mabbs, and T. J. King, *J. Chem. Soc., Chem. Commun.*, 740 (1978); (b) G. Christou, C. D. Garner, and F. E. Mabbs, *Inorg. Chim. Acta*, **28**, L189 (1978).

(5) G. Christou, G. D. Garner, F. E. Mabbs, and M. G. B. Drew, *J. Chem. Soc., Chem. Commun.*, 91 (1979).

(6) (a) D. Coucouvanis, N. C. Baenziger, E. D. Simhon, P. Stremple, D. Swenson, A. Kostikas, A. Simopoulos, V. Petrouleas, and V. Papaefthymiou, *J. Am. Chem. Soc.*, **102**, 1730 (1980); (b) *ibid.*, **102**, 1732 (1980).

(7) W. G. Zumft, *Eur. J. Biochem.*, **91**, 354 (1978).

(8) K. H. Schmidt and A. Müller, *Coord. Chem. Rev.*, **14**, 115 (1974).

(9) A. Müller and S. Sarkar, *Angew. Chem., Int. Ed. Engl.*, **16**, 705 (1977).

(10) K. P. Callahan and P. A. Piliero, *J. Chem. Soc., Chem. Commun.*, 13 (1979).

(11) A. Müller, R. Jostes, V. Flemming, and R. Potthast, *Inorg. Chim. Acta*, **44**, L33 (1980).

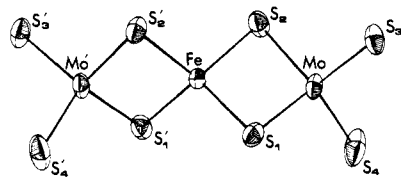


Figure 1. Structure and labeling of the $[(\text{MoS}_4)_2\text{Fe}]^{3-}$ anion. Thermal ellipsoids are drawn by ORTEP (C. K. Johnson, ORNL-3794, Oak Ridge National Laboratory, Oak Ridge, TN, 1965) and represent the 50% probability surfaces. The connecting lines between the Fe and Mo atoms do not imply bonding. Instead, they emphasize the bend in the Mo-Fe-Mo array.

trated dimethylformamide (DMF) solution of Cat_2MoS_4 with a CH_3CN solution of $(\text{Cat})[\text{Fe}(\text{S}_2\text{COC}_2\text{H}_5)_3]^{12}$ ($\text{Cat} = \text{Me}_4\text{N}^+$, Et_4N^+) affords violet crystals of these "salts", which can be recrystallized from DMF solutions upon the addition of ether. All attempts to obtain single crystals, suitable for X-ray diffraction with either the Et_4N^+ or the Me_4N^+ counterions, failed. A cation exchange was attempted by adding a warm aqueous solution of bis(triphenylphosphine)iminium chloride, $(\text{PPh}_3)_2\text{NCl}$, to a DMF solution of $(\text{Et}_4\text{N})_3[(\text{MoS}_4)_2\text{Fe}]$. Violet plates of the mixed cation salt $[(\text{PPh}_3)_2\text{N}]_2(\text{Et}_4\text{N})[(\text{MoS}_4)_2\text{Fe}]$ were formed and isolated upon cooling. Single crystals of the bis DMF solvate¹³ were obtained by the slow diffusion of ether to a DMF solution of this complex (I) [Anal. Calcd for $\text{FeMo}_2\text{S}_8\text{C}_{72}\text{H}_{60}\text{N}_2\text{P}_4\text{C}_6\text{H}_{20}\text{N}\cdot\text{C}_6\text{H}_{14}\text{O}_2\text{N}_2$ (M_w 1857.9): C, 55.59; H, 5.11; N, 3.77; P, 6.67; S, 13.80; Fe, 3.01; Mo, 10.33. Found: C, 55.0; H, 5.01; N, 3.60; P, 6.41; S, 14.05; Fe, 3.45; Mo, 9.76]. The visible spectrum (DMF) of this paramagnetic¹⁴ compound ($\mu_{\text{eff}}^{\text{corr}} = 3.85 \mu_B$ at 303 K) is characterized by absorptions at 650 (sh), 583 (ϵ 8360), 510 (18 254), 409 (9848), 375 (sh), 348 (25 546), and 290 (21 350) nm. An $S = 3/2$ ground state is suggested by the magnetic moment and by the simple Curie-Weiss magnetic behavior evident in the temperature dependence of the magnetic susceptibility.

The infrared spectrum of I (KBr disk) shows absorptions at 495, 472, and 438 cm^{-1} , which can be attributed to the terminal (495, 472 cm^{-1}) and bridging (438 cm^{-1}) Mo-S vibrations of the MoS_4^{2-} bidentate chelate.¹³ While this manuscript was in preparation, McDonald and co-workers informed us of the synthesis of the same $[(\text{MoS}_4)_2\text{Fe}]^{3-}$ anion obtained by a similar synthetic approach.¹⁶ In their study, they obtained the EPR spectrum of this complex anion which showed g values at 4.6, 3.3, and 2.0 and was attributed to a $S = 3/2$ ground state. These results complement our magnetic susceptibility measurements which also indicate the presence of three unpaired electrons.

Single-crystal, X-ray-diffraction, and intensity data on I were collected on a Picker-Nuclear FACS-I automatic diffractometer by using a θ - 2θ scan technique.¹⁷ The data corrected for Lorentz, polarization, and absorption effects were used for the solution of the structure by conventional Patterson and Fourier techniques. Refinement by full-matrix least-squares methods has progressed to a conventional R value of 0.073 by using isotropic thermal parameters for the carbon atoms of the $(\text{Ph}_3\text{P})_2\text{N}^+$ cations and anisotropic thermal parameters for all other atoms. The hydrogen atoms for the Et_4N^+ cation and for the two DMF solvent molecules

(12) D. G. Holah and C. N. Murphy, *Can. J. Chem.*, **49**, 2726 (1971). Very likely, the xanthate ligand serves as the reducing agent in this reaction.

(13) The DMF solvent molecules and the Et_4N^+ cation were detected by NMR spectroscopy in dimethyl- d_6 sulfoxide. Integration of the signals and comparison to the signal of the $(\text{Ph}_3\text{P})_2\text{N}^+$ cation verified the stoichiometry suggested by the analytical data and subsequently shown by the X-ray structure determination.

(14) The magnetic moment was determined in $\text{Me}_2\text{SO}-d_6$ solution by an NMR technique.

(15) A. Müller, E. Ahlborn, and H. H. Heinsen, *Z. Anorg. Allg. Chem.*, **386**, 102 (1971).

(16) J. W. McDonald, G. D. Friesen, and W. E. Newton, *Inorg. Chim. Acta*, in press.

(17) Crystal and refinement data for $[(\text{PPh}_3)_2\text{N}]_2(\text{Et}_4\text{N})[(\text{MoS}_4)_2\text{Fe}]\cdot 2\text{DMF}$: $a = 12.649$ (3), $b = 34.179$ (6), $c = 10.870$ (2) Å; space group $F2_22_2$; $Z = 2$; $d_{\text{calcd}} = 1.313 \text{ g/cm}^3$, $d_{\text{obsd}} = 1.33 \text{ g/cm}^3$; crystal dimensions (cm) $0.044 \times 0.010 \times 0.085$; $2\theta_{\text{max}} 45^\circ$ (Mo radiation); $F^2 > 3\sigma(F^2)$, 2967 reflections used; 3416 unique reflections; 316 parameters.

Table I. Structural Parameters^a in the $[(\text{MoS}_4)_2\text{Fe}]^{3-}$ (I), $[(\text{PhS})_2\text{FeS}_2\text{MoS}_2]^{2-}$ (II), and $[\text{Cl}_2\text{FeS}_2\text{MoS}_2\text{FeCl}_2]^{2-}$ (III) Anions

	I	II ^b	III ^{c,d}
bond lengths, Å			
Fe-Mo	2.740 (1)	2.750 (4)	2.775 (6)
Mo-S ₁	2.260 (4)	2.247 (6)	
Mo-S ₂	2.251 (5)	2.245 (6)	2.204 (5)
Mo-S ₃	2.169 (5)	2.148 (6)	
Mo-S ₄	2.173 (5)	2.159 (6)	
Fe-S ₁	2.245 (4)	2.242 (7)	
			2.295 (5)
Fe-S ₂	2.268 (4)	2.258 (7)	
S ₁ -S ₂	3.579 (5)	3.571 (8)	3.543 (6)
S ₂ -S ₂ '	3.816 (5)		
S ₁ -S ₁ '	3.791 (6)		
bond angles, deg			
Mo-Fe-Mo	172.64 (6)		
S ₁ -Fe-S ₂	104.9 (2) ^e	102.9 (3)	101.0 (1)
S ₁ -Mo-S ₂	105.0 (2) ^f	104.5 (3)	107.1 (1)
Fe-S ₁ -Mo	74.90 (12)	75.5 (2) ^d	76.05 (9)
Fe-S ₂ -Mo	74.64 (13)		

^a For all structures, the reported structural parameters are in analogous reference to the labeling shown in Figure 1. ^b From ref 18. ^c From ref 6b. ^d Mean values; the standard deviation from the mean is in parentheses. ^e Range in $\text{S}_1\text{-Fe-S}_j$ angles is 104.9–115.2°. ^f Range in $\text{S}_1\text{-Mo-S}_j$ angles is 105.0–112.9 (3)°.

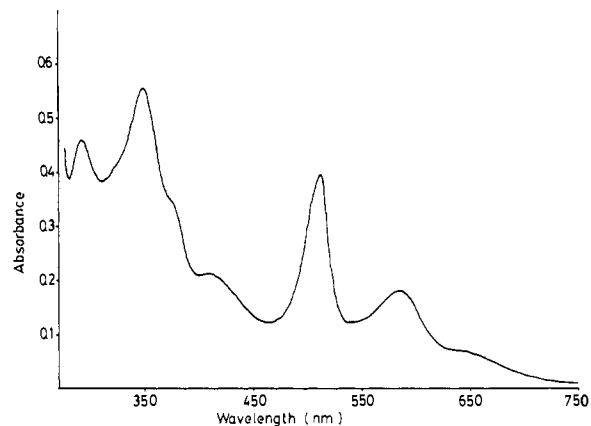


Figure 2. The visible spectrum of $[(\text{Ph}_3\text{P})_2\text{N}]_2(\text{Et}_4\text{N})[(\text{MoS}_4)_2\text{Fe}]$ in DMF.

have not been included in the refinement process as yet. The structure of the anion (Figure 1) shows the tetrahedrally coordinated Fe atom (on a crystallographic 2-fold axis) bound by two MoS_4^{2-} bidentate chelates. A slight bend in the Mo-Fe-Mo backbone [Mo-Fe-Mo angle 172.64 (6)°] could arise from packing forces and particularly from the close proximity of several cation hydrogen atoms to S_4 . Selected structural parameters in the $[(\text{MoS}_4)_2\text{Fe}]^{3-}$ anion are shown in Table I and are compared to corresponding values in the structures of the $[(\text{PhS})_2\text{FeS}_2\text{MoS}_2]^{2-}$ (II)¹⁸ and $[\text{Cl}_2\text{FeS}_2\text{MoS}_2\text{FeCl}_2]^{2-}$ (III) complexes. The FeS_2Mo unit in I is essentially planar and similar to the one found in II. In particular, the Fe-S bond length in I [2.256 (11) Å] is well within 1σ from that of II [2.250 (8) Å]. The Mo-S terminal bond length in I [2.171 (5) Å] is somewhat longer than the one found in II [2.153 (6) Å] and appears closer to the value reported for the Mo-S bond in MoS_4^{2-} (2.18 Å).¹⁹ The bridging Mo-S bond length, at 2.256 (5) Å for I, is quite similar to that of the corresponding bond in II [2.246 (6) Å]. The crystallographic results, and in particular the rather short Fe-S bonds, suggest that the reduction is not centered on the iron atom. Instead, it is more likely that a delocalization of charge to the MoS_4^{2-} "ligands" has occurred. The rather long terminal Mo-S

(18) D. Coucouvanis, E. D. Simhon, D. Swenson, and N. C. Baenziger, *J. Chem. Soc., Chem. Commun.*, 361 (1979).

(19) P. A. Koz'min and Z. V. Popova, *Zh. Strukt. Khim.*, **12**, 99 (1971).

bonds in I may reflect a weakening of the Mo-S_t π bonds and a higher electron density at the terminal sulfur atoms.⁹

The contention that the reduction is not centered on the iron atom in I is strongly supported by the Mössbauer data. Preliminary results of the Mössbauer spectrum of I, in liquid N₂, show an isomer shift (IS) of 0.38 (3) mm/s vs. Fe and a quadrupole splitting of 1.04 (3) mm/s.²⁰ The low value of the IS in I indicates that the formal d orbital occupancy of the Fe center is smaller than that expected for either a 1+ or even a 2+ oxidation state. The cyclic voltammogram of I²¹ shows a quasi-reversible reduction at ~-1.8 V and an irreversible oxidation at ~-0.10 V. Essentially the same results were reported previously by McDonald and co-workers.¹⁶ The irreversibility of the oxidation wave clearly shows the instability and perhaps raises doubts as to the actual existence of a discrete [(MoS₄)₂Fe]²⁻ complex anion.

A comment should be made concerning the recently reported [Fe₄Mo₄S₂₀]⁶⁻ cluster.²² The published electronic spectrum of this compound appeared to us similar, if not identical, to that of I (Figure 2). We repeated the synthesis of the "[Fe₄Mo₄S₂₀]⁶⁻" anion as described in the literature. The Et₄N⁺ salt of the product we obtained was found X-ray isomorphous to the corresponding derivative of I. Furthermore, the energies and absolute intensities of the electronic absorptions of the two compounds were virtually identical. On the basis of these results and similarities in the infrared and Mössbauer spectra between the two compounds, we propose that the "[Fe₄Mo₄S₂₀]⁶⁻" anion is in fact the [Fe-(MoS₄)₂]³⁻ complex anion.

In conclusion, the facility of the Fe-MoS₄ chromophore to accept electrons makes this moiety ideally suited for the storage of electrons or perhaps even the relay of electrons under appropriate conditions. The reactivity of I is presently under study.

Acknowledgment. This work has been generously supported by grants from the National Science Foundation (CHE-79-0389) and the National Institutes of Health (GM-26671-01). The computing expenses have been covered by grants from The University of Iowa Graduate College.

Supplementary Material Available: Tables of atomic positional and thermal parameters and a list of observed and calculated structure amplitudes (14 pages). Ordering information is given on any current masthead page.

(20) D. Niarchos, personal communication.

(21) Cyclic voltammetry was conducted in CH₃CN (0.1 M) in tetrabutylammonium perchlorate on a Pt electrode vs. a saturated calomel reference electrode.

(22) H. C. Silvis, R. H. Tieckelmann, and B. A. Averill, *Inorg. Chim. Acta*, **36**, L423 (1979).

D. Coucouvanis,* E. D. Simhon, N. C. Baenziger

*Department of Chemistry, University of Iowa
Iowa City, Iowa 52242*

Received April 29, 1980

Exceptional Micellar Stereoselectivity in Esterolysis Reactions: The Micelle-Enzyme Analogy

Sir:

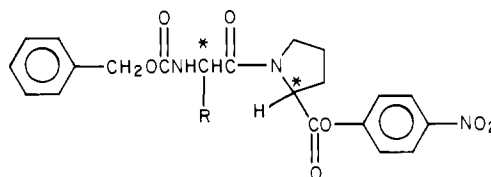
The kinetic analogy between micelle- and enzyme-catalyzed reactions is well-known and extensively documented, particularly for esterolyses.¹ Impressive micellar rate enhancements attend the cleavage of activated esters by, e.g., imidazole- or thiol-functionalized surfactants.²⁻⁴ However, progress has been less

rapid in micellar control of esterolysis stereochemistry. Only modest enantioselectivity (~11%) was reported for cleavage of the enantiomeric *p*-nitrophenyl α-methoxyphenylacetates with *l*-*N*-dodecyl-*N*-methylephedrinium bromide micelles;⁵ similar experiments with other chiral ammonium⁶ or sulfoxonium⁷ salts were unsuccessful.

The situation is somewhat better with various enantiomeric *N*-protected *p*-nitrophenyl amino acid ester substrates: enantioselectivities up to ~3:1 have been observed in esterolyses catalyzed by chiral histidine-functionalized surfactant micelles,⁸ or by *N*^α-acylhistidines^{9a} or *l*-alanillylaurylamide^{9b} solubilized in, e.g., cetyltrimethylammonium (CTA) micelles. Even here, however, mechanistic details remain unclear, and related experiments with histidine or cysteine surfactants afforded insignificant enantioselectivity.¹⁰ Not surprisingly, recent reviews of micellar catalysis have criticized the micelle-enzyme analogy, particularly citing the lack of substantial, predictable stereochemical control.^{11,12}

In view of the currently modest experimental success,⁵⁻¹⁰ and the pessimistic overall assessment,^{11,12} we think it appropriate to disclose exceptional micellar stereoselectivity in the cleavage of diastereomeric dipeptide *p*-nitrophenyl (PNP) esters.¹³ Our best cases are an order of magnitude greater than previous examples of micellar esterolytic stereoselectivity. Moreover, the new results can be fitted to a rational, predictive model.

Substrates I-V were generally synthesized by mixed anhydride coupling of the appropriate *D*- or *L*-benzyloxycarbonyl *Z*-protected amino acid to *L*-proline PNP ester in cold CH₂Cl₂ or THF.¹⁴ The



I, R = CH₃ [(*Z*)-Ala-Pro-PNP]

II, R = CH₂C₆H₅ [(*Z*)-Phe-Pro-PNP]

III, R = CH₂-(3-indolyl) [(*Z*)-Trp-Pro-PNP]

IV, R = CH₂CH(CH₃)₂ [(*Z*)-Leu-Pro-PNP]

V, R = CH(CH₃)₂ [(*Z*)-Val-Pro-PNP]

n-C₁₆H₃₃N⁺(CH₃)₂CH₂CH₂SH,Cl⁻

VI (16-SH)

products were purified by crystallization and/or chromatography

(3) Moss, R. A.; Bizzigotti, G. O.; Huang, C.-W. *J. Am. Chem. Soc.* **1980**, *102*, 754. Moss, R. A.; Bizzigotti, G. O.; Lukas, T. J.; Sanders, W. J. *Tetrahedron Lett.* **1978**, 3661. Anoardi, L.; Fornasier, R.; Sostero, D.; Tonellato, U. *Gazz. Chim. Ital.* **1978**, *108*, 707.

(4) Moss, R. A.; Lukas, T. J.; Nahas, R. C. *J. Am. Chem. Soc.* **1978**, *100*, 5920.

(5) Bunton, C. A.; Robinson, L.; Stam, M. F. *Tetrahedron Lett.* **1971**, 121.

(6) Moss, R. A.; Sunshine, W. L. *J. Org. Chem.* **1974**, *39*, 1083.

(7) Jugé, S.; Meyer, G. *Tetrahedron* **1980**, *36*, 959.

(8) Brown, J. M.; Bunton, C. A. *J. Chem. Soc., Chem. Commun.* **1974**, 969.

(9) (a) Ihara, Y. *J. Chem. Soc., Chem. Commun.* **1978**, 984. Yamada, K.; Shosenji, H.; Ihara, H. *Chem. Lett.* **1979**, 491. Yamada, K.; Shosenji, H.; Ihara, H.; Otsubo, Y. *Tetrahedron Lett.* **1979**, 2529. (b) Ihara, H.; Ono, S.; Shosenji, H.; Yamada, K. *J. Org. Chem.* **1980**, *45*, 1623.

(10) Moss, R. A.; Lukas, T. J.; Nahas, R. C. *Tetrahedron Lett.* **1977**, 3851. Moss, R. A.; Nahas, R. C.; Lukas, T. J. *Ibid.* **1978**, 507.

(11) (a) Bunton, C. A. in "Application of Biomedical Systems in Chemistry"; Jones, J. B., Ed.; Wiley: New York, 1976; Part II, pp 731-814. (b) Bunton, C. A.; Romsted, L. S. "Chemistry of Functional Groups, Supplement B, Chemistry of Acid Derivatives"; Patai, S., Ed.; Wiley: New York, 1979; Part 2, pp 945-1020. (c) Bunton, C. A. *Pure Appl. Chem.* **1977**, *49*, 969. (d) *Catal. Rev.-Sci. Eng.* **1979**, *20*, 1.

(12) See especially ref 11d, pp 46-47.

(13) We previously reported kinetic stereoselectivities of 3.9-4.3 in micellar esterolysis of (*Z*)-(L- or D)-Ala-L-Pro-PNP by thiol-functionalized surfactants: Moss, R. A.; Lee, Y.-S.; Lukas, T. J. *J. Am. Chem. Soc.* **1979**, *101*, 2499.

(14) (a) Substrates IV were prepared by DCC/HOBt coupling of (*Z*)-Leu to Pro-OMe. Controlled hydrolysis then gave (*Z*)-Leu-Pro-OH, which was coupled to *p*-nitrophenol with DCC. For procedures, see: McDermott, J. R.; Benoiton, N. L. *Can. J. Chem.* **1973**, *51*, 2559. Bodanszky, M.; Du Vigneaud, V. *J. Am. Chem. Soc.* **1959**, *81*, 5688. (b) Details will appear in a full paper, and in the Ph.D. Dissertation of Y.-S. Lee

(1) (a) Cordes, E. H., Ed. "Reaction Kinetics in Micelles", Plenum Press: New York, 1973. (b) Fendler, J. H.; Fendler, E. J. "Catalysis in Micellar and Macromolecular Systems", Academic Press: New York, 1975.

(2) Moss, R. A.; Nahas, R. C.; Ramaswami, S. *J. Am. Chem. Soc.* **1977**, *99*, 627. Tonellato, U. *J. Chem. Soc., Perkin Trans. 2* **1976**, 771.